Application of Artificial Damping Method to Practical Instability Problems

Takaya Kobayashi, and Yasuko Mihara

Mechanical Design & Analysis Corporation

***Abstract**: The buckling of a real, thin-walled shell is typically a local phenomenon, and it may be triggered by a small, local disturbance. Regarding these problems, a very slight imperfection can be the starting point from which local deformation is initiated and developed and, consequently, overall structural stability is lost. Therefore, it has been very difficult to pursue an analysis using the conventional approach, which is typically represented by the arc-length method. In this study, we provide an explanation for the artificial damping method from which we can overcome the difficulty in performing the analysis due to local instability.*

***Keywords**: Buckling, Elastic Stability, Shell, Artificial Damping.*

1. Introduction

Geometrically nonlinear static problems sometimes involve buckling or collapse behavior, in which the load-displacement response shows a negative stiffness and the structure must release strain energy to remain in equilibrium. Several approaches can be used to model such behavior. Among them, path tracing, based on the arc-length method, is the most fundamental procedure. This method is used for cases in which the loading is proportional, that is, in which the load magnitudes are governed by a single scalar parameter. If the analysis process traces unstable paths under the global load-displacement response with negative stiffness, the arc-length method is effectively usable. However, if the instability is localized (e.g., surface wrinkling, material instability, or local buckling), there will be a local transfer of strain energy from one part of the model to the neighboring parts, and global solution methods may not work. This class of problems must be solved either dynamically or with the aid of artificial damping.

This paper provides an explanation for the artificial damping method, taking the snap-through buckling of a two-bar truss as an example. The analytical results for the problem using the arc-length method, the static artificial damping method, and the implicit dynamic method are compared. The artificial damping method demonstrates the path-tracing performance to provide a “stable” equilibrium solution within the static analysis, which will make useful theoretical options available for local buckling problems. This paper also describes the practical examples of the application of the artificial damping technique: the generation of singularities in large-deformed shells, as well as wrinkling of thin-walled materials.

2. Artificial damping method

The artificial damping method is a technique used to achieve total energy balance in static analysis, compensating for strain energy changes due to local elastic instability. In the present study, Abaqus (Dassault, 2013), the general-purpose finite element code, was used due to its powerful nonlinear capability to overcome the analytical instabilities encountered in thin-shell problems, while the artificial damping method or its comparable quasistatic capabilities are available in other codes, such as ADINA, ANSYS, and Marc. Abaqus provides an automatic mechanism for stabilizing unstable quasi-static problems through the automatic addition of volume-proportional damping to the model. Via Equation (1), viscous forces are added to the global equilibrium equations, as shown in Equation (2):

$$\mathbf{F}_{\mathrm{v}} = c\mathbf{M}^{*}\mathbf{v} \tag{1}$$

$$\mathbf{P} - \mathbf{Q} - \mathbf{F}_{\mathrm{v}} = \mathbf{0} \tag{2}$$

where $\mathbf{M}^{*}$ is an artificial mass matrix calculated with unity density, c is a damping factor, $\mathbf{v} = \Delta\mathbf{u}/\Delta t$ is the vector of nodal velocity, $\Delta\mathbf{u}$ is the vector of incremental displacement, Δt is the increment of time (which may or may not have a physical meaning in the context of the problem being solved), $\mathbf{P}$ is the total applied load, and $\mathbf{Q}$ is the internal force. When local instability occurs, the deformation rate of that portion begins to increase, and locally released strain energy is dissipated due to the appended damping effect. Consequently, quasi-static analysis makes it possible to treat the problems involved in local instability.

Empirically, as is the case in general, moderate stabilizing can be achieved by adjusting the damping factor c in Equation (1) so that the total dissipated energy does not exceed 1–10% of the total strain energy. In terms of Abaqus use, the damping factor c is specified by an indirect input parameter called “the dissipated energy fraction,” which is the ratio of the allowable incremental damping energy (the dissipated energy for a given increment) to the total strain energy. The fraction has a default value of 2.E-4. The damping factor for each individual element is adjusted to meet the requirements at both the global and the local element level. However, since the artificial damping energy is classified as non-conservative, the resultant energy always increases, while the strain energy may decrease. Therefore, the above-mentioned treatment is just a target and can be corrected in some situations, such as when there is rigid body motion or when significant non-local instability occurs. In such cases, the damping factor is chosen such that the average element damping matrix component, divided by the step time, is equal to the average element stiffness matrix component multiplied by the dissipated energy fraction.

Based on our practical experience, lowering the dissipated energy fraction to 1/100–1/1,000 of the default value (2.E-4) provides highly sensitive analytical performance (Kobayashi, 2012). This technique is useful, for instance, to achieve precise expressions of the mode jumping along with the sharp dropping of the load for thin shell problems.

3. Snap-through buckling of two-bar truss

To ensure the performance of the artificial damping method, a truss structure was analyzed. Figure 1 shows the analysis model. The model is assembled from two truss members that are moderately sloped to form an upwards convex frame. A downward point load Λp is applied so that the structure can exhibit snap-through buckling, where Λ is the load proportionality factor. The total potential energy Π can be expressed as shown in Equation (3). The terms on the right-hand side of the equation represent the strain energy and the load potential.

$$\Pi(U_1, U_2, \Lambda) = \frac{1}{2} L_0 EA\{(\varepsilon_1)^2 + (\varepsilon_2)^2\} - \Lambda p U_2 \tag{3}$$

where

L_0: initial length of each truss (W = 1000 mm, H = 100 mm),

A: cross-sectional area of a truss member (100 mm^2),

E: Young's modulus (2.E5 MPa), p: Unit load (1 N)

Setting the derivative of Π with respect to U_2 being zero, as per Equation (4), the equilibrium path in the load-displacement space can be obtained based on the stationary principle of potential energy.

$$\left.\frac{\partial \Pi}{\partial U_2}\right|_{U_1=0} \equiv L_0 EA\left(\varepsilon_1 \frac{\partial \varepsilon_1}{\partial U_2} + \varepsilon_2 \frac{\partial \varepsilon_2}{\partial U_2}\right) - \Lambda p = 0 \tag{4}$$

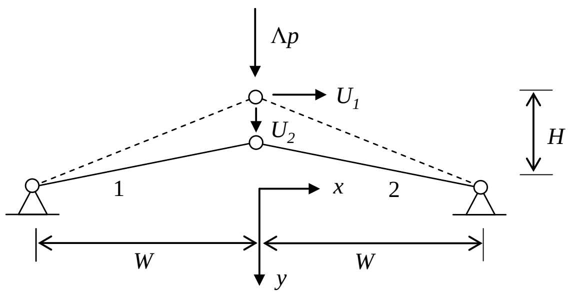

Figure 1. Two-bar truss problem.

Figure 2(a) shows the obtained load-displacement curve. Obviously, a negative stiffness is generated. This problem represents a typical case of snap-through buckling. Figure 2(b) shows the energy variation. The responses of the strain energy and the external work are identical because the problem is solved as a static equilibrium.

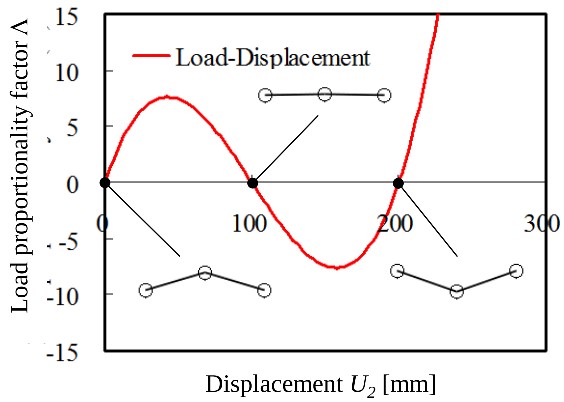

(a) Load-displacement

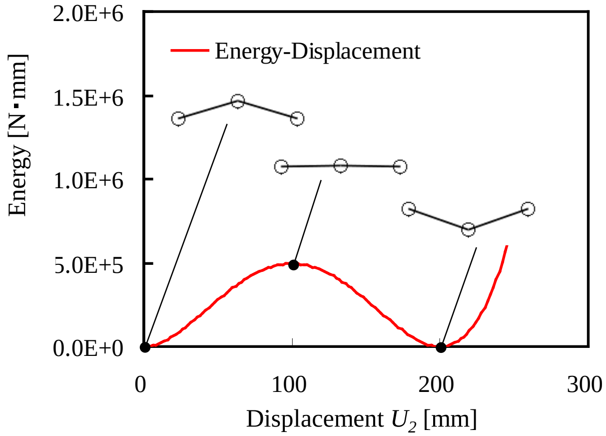

(b) Energy-displacement

Figure 2. Static equilibrium path of two-bar truss (Theory).

While the paths, shown in Figure 2(a) and (b), can be directly derived by applying the arc-length method, the artificial damping method was applied to the problem. As seen in Figure 3(a), beyond the maximum load (Point A), the deformation path jumps to the next stable path (Point B), keeping the same magnitude without any further reduction from the maximum value. In the real world, a similar snap-through behavior should be observed. The change in energy is shown in Figure 3(b). Irrespective of the occurrence of this snap-through behavior, the deformation of the truss members will progress in the same manner, and thus, the change in the strain energy should follow the same path, as shown in Figure 2(b). However, the external work appears to increase monotonously because no reduction in the load occurs. As indicated in Figure 3(b), the difference between the external work and the strain energy corresponds to the resultant energy produced by the artificial damping effect. As mentioned above, since the artificial damping energy is classified as non-conservative, the resultant energy (white triangle marks in Figure 3(b)) represents the cumulative energy generated from the artificial damping. The artificial damping energy is provided to stabilize the truss motion as the path jumps from Point A to Point B. Once the deformation reaches the stable post-buckling path (Point B), no further artificial damping energy is provided.

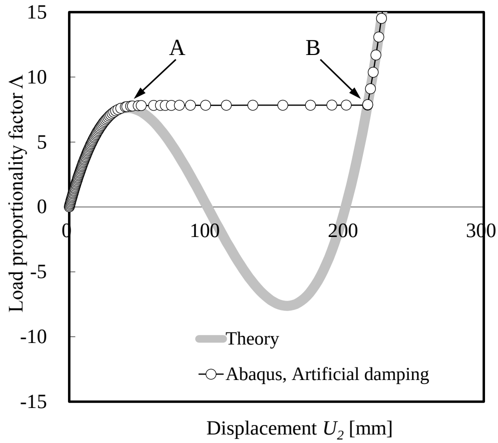

(a) Load-displacement

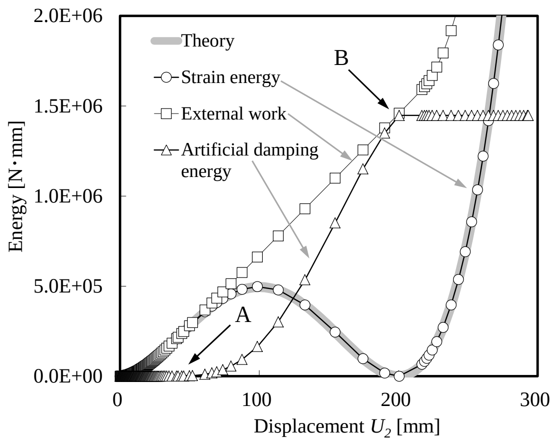

(b) Energy-displacement

Figure 3. Snap-through response of two-bar truss (Artificial damping method).

Figures 4(a) and (b) show the analytical results for the two-bar truss problem using dynamic response analysis. In this case, the implicit dynamic procedure (the HHT method in Abaqus, similar to the Newmark-β method) was applied. Note that the explicit procedure will provide identical results for this class of problems. As shown in Figure 4(a), snap-through behavior similar to that seen in the artificial damping method case (Figure 3(a)) occurs; however, overshooting and

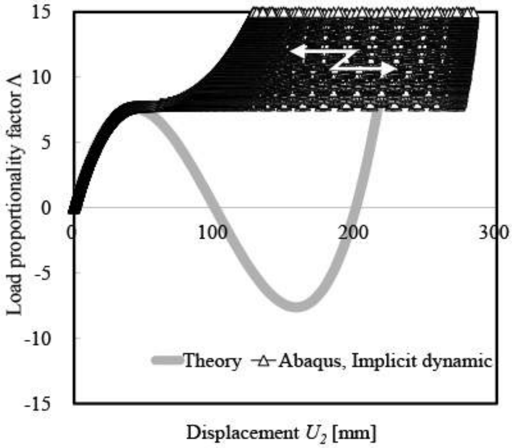

(a) Load-displacement

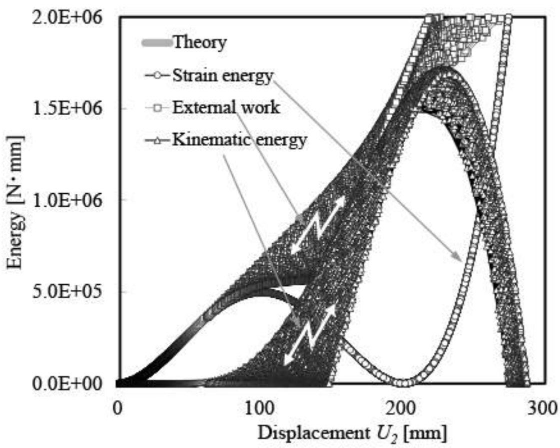

(b) Energy-displacement

Figure 4. Snap-through response of two-bar truss (Implicit dynamic method).

oscillation are clearly observed in the truss deformation. The oscillation never decays, unless damping effects are specified for the problem. However, in Figure 4(a), the oscillation diminishes in amplitude while shifting its center position to the right in the figure because the applied load is set to monotonically increase and the geometrically nonlinear option is invoked in the analysis. Note that the default setting for the HHT method of Abaqus includes a slight numerical damping to provide desirable stabilizing effects. The default setting was not ruled out in this case.

Figure 4(b) shows the energy variation. The response of the strain energy is identical with the above-mentioned cases because the strain energy is determined by the truss deformation even though the truss is in dynamic motion. The difference between the external work and the strain energy is the kinematic energy produced by the inertia effect. The snap-through jump is a consequence of the sudden release of stored elastic strain energy and its transformation into kinetic energy. Since the truss oscillates between the top dead center and the bottom dead center, the kinematic energy varies between 0 and 0, straddling the maximum. An animation file demonstrating the energy variation illustrated in Figure 4(b) is available on the author's website (Mechanical Design & Analysis Corporation). This will be helpful in providing a visual understanding of the energy balance.

The artificial damping energy curve (Figure 3(b)) and the kinematic energy curve (Figure 4(b)) are equivalent in the path- jumping region (around $50 \leq U_2 \leq 200$ mm), except for the dynamic oscillation superimposed on the kinematic energy curve. In real cases, the energy generated by the artificial damping is equivalent to the energy released as the inertia effect. Specifically, replacing the kinetic energy with artificial damping energy makes it possible to analyze the unstable phenomenon stably in order to obtain the equilibrium solution within the static analysis. Because the artificial damping can be introduced in proportion with the rate generated locally in the analysis model, as per Eq. (1) and Eq. (2), these characteristics can be applied to the phenomenon in a locally unstable situation, which the arc-length method would handle poorly. Practical cases to which the artificial damping method can be applied are shown in the following section.

4. Applications of artificial damping method

4.1 Elastic cylindrical shells under axial compression

The buckling of axially compressed cylindrical shells is known to be sensitive to imperfections, as is the buckling of spherical shells under external pressure. Regarding these problems, a very slight imperfection can be the starting point from which local deformation is initiated and developed and, consequently, overall structural stability is lost. To demonstrate the applicability of the artificial damping method, the authors traced this successive buckling of the elastic cylindrical shells under axial compression (Kobayashi 2012). The study accomplished a fully automatic and seamless simulation of successive path jumpings in the deep post-buckling region and showed good agreement with Yamaki's experimental results (1984) and Esslinger's high-speed photography (1970). The main points of the analytical techniques may be summarized as follows:

- Application of high performance shell elements (S4R in Abaqus);
- Composition of high-resolution mesh (with a maximum element length no longer than $0.3(Rt)^{½}$);
- Appropriate provision of initial imperfection;
- Achievement of total energy balance, providing compensation for strain energy changes due to local elastic instability.

Figure 5. Beverage can under axial compression (Mihara and Kobayashi, 2008).

4.2 Material-related instability problems for inelastic thin shells

Whereas the sudden release of stored elastic strain energy provides the inertia effect during elastic buckling, the inelastic material properties typically represented by plasticity and viscoelasticity can also affect the buckling behavior. Taking the viscoelasticity as an example, this kind of material-related instability may occur in the formation process of thin-walled structures, such as the blow-forming of plastic containers or the formation of polymer thin films. Regarding these problems, the authors performed experimental and analytical investigations of viscoelastic cylindrical shells under axial compression (Kobayashi, 2016), as well as wrinkling during elastoplastic cup drawing (Oide, 2016). Plastic and/or viscoelastic material properties actually provide stabilizing effects regarding dynamic aspects. However, in a static scheme, the rapid decrease in elastic modulus may cause the loss of structural stability. The artificial damping method also overcomes analytical difficulties due to material-related instability because the instantaneous stiffness change can be reflected in the global equilibrium equations with appropriately adjusting the damping force so as to correspond to the states of the local and individual instabilities in the model. While explicit dynamic codes have been conventionally used in the field of sheet metal forming analysis, one of the practical advantages of using implicit codes is that they make it possible to calculate eigenmodes at any midpoint in the analysis. Incidentally, the explicit dynamic method is poorly suited to lengthy events (empirically more than one second).

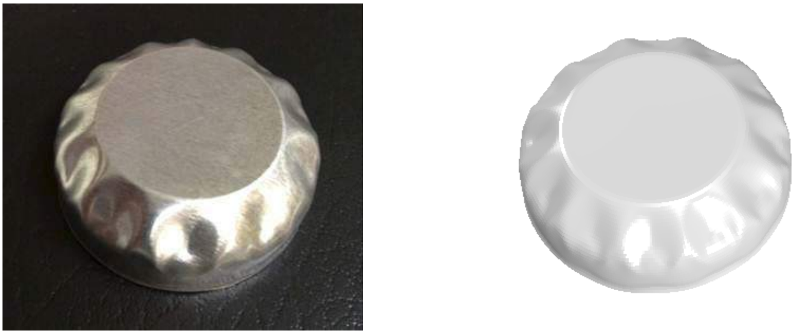

Experiment FEM

Figure 6. Draw cup with wrinkles.

4.3 Local buckling in microscopic structures

The athletic footwear industry has made steady progress in technological innovations to give the athlete a greater running experience. Modern sport shoes are designed to attenuate the ground reaction forces, mainly through deformation of the midsole, which is typically made of ethylene vinyl acetate (EVA) foam. Figure 7 (a) shows an SEM image of EVA foam presented by ASICS Institute of Sport Science (Tateishi and Nishiwaki, 2011). The EVA foam has a closed cell structure composed of a polymer wall with a thickness of 5–10 μm and cell diameters of 50–500 μm. A one-shot press-molding process, in which the preformed compounds were composed of organic peroxide as a cross-linking agent and azodicarbonamide as a chemical bowing agent, was applied to fabricate the EVA foam.

Figure 7 (b) shows tomograms and a three-dimensional rendering view of an undeformed EVA foam specimen. Simpleware, the 3D image visualization and processing software, was used for its practical capability of reconstructing 3D finite element mesh from tomography data. The cell (dark domain) and the cell wall (white linear structure) are clearly depicted. However, troublesome manual operations such as eliminating the fragments of polymer by hand were required to finish the mesh surface because the foam cells originally have rough surfaces resulting from the chemical reaction foaming process. Poor quality elements with micro-sized edges could not be completely removed from the model. The finite element model was composed of around 350,000 C3D4H (first-order hybrid tetrahedron) mesh. The material property of the cell wall was assumed to be hyperelastic with an initial elastic coefficient of 30 MPa. The effect of gas in the cells could be ignored.

Figure 8 shows the stress-strain behaviors under uniaxial compression. The compressive response of polymer foam can be classified into elastic, plateau, and densification regions. The plateau is associated with elastic buckling of the cell wall. The shock-absorbing property predominantly depends on the amount of deformation energy accumulated in the plateau region. When the cells have almost completely collapsed, opposing cell walls touch and further strain compresses the solid itself, giving the final region of rapidly increasing stress, referred to as densification. The analytical result shows good agreement with the experimental observations.

Figure 9 (a) shows the local buckling behavior observed in the plateau region. As seen in the figure, the artificial damping method in Abaqus captured clear views of the local buckling of cell walls. Figure 9 (b) shows similar experimental results from the reference (Phelps, 2005).

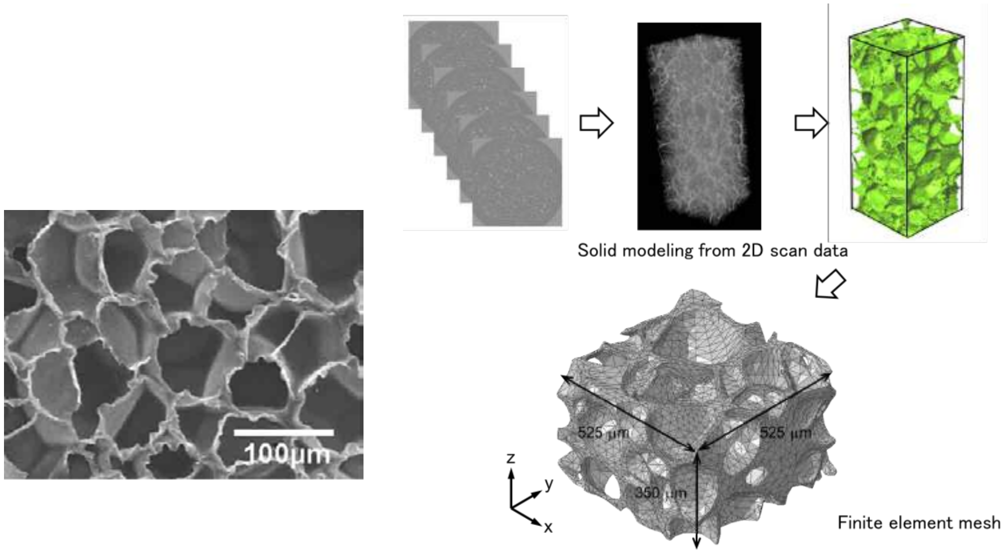

(a) **(b)**

Figure 7. 3D modeling of Ethylene-vinyl acetate (EVA) foam. (a) SEM image; (b) Reconstructing 3D finite element mesh from tomography data.

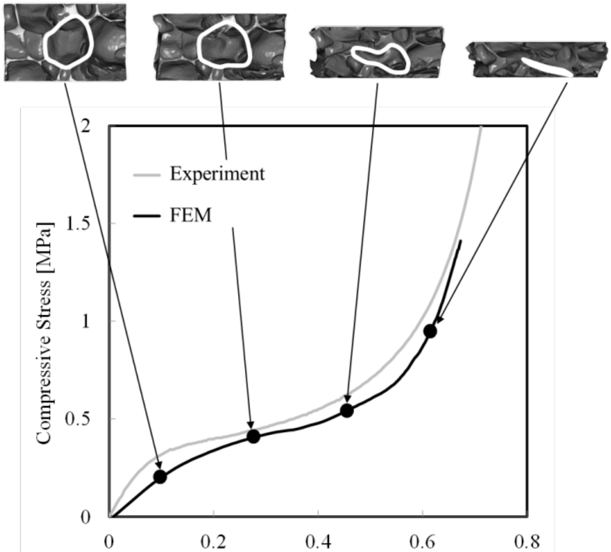

Figure 8. Stress-strain curves of EVA foam.

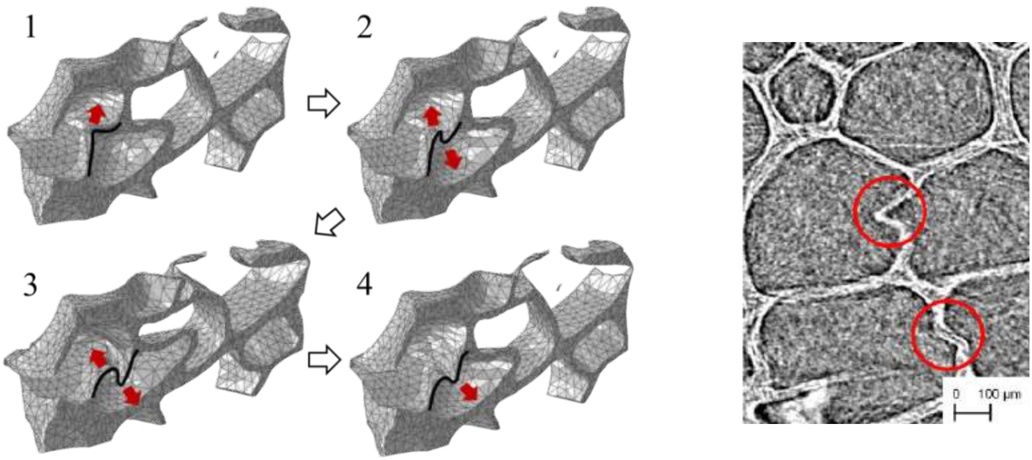

(a) **(b)**

Figure 9. Local buckling of cell walls.

(a) This study (Abaqus, artificial damping); (b) Reference (Phelps, 2005)

5. Conclusion

In designing a modern lightweight structure, it is of technical importance to ensure its safety against buckling under the applied loading conditions. This study presents the application of the artificial damping method to practical instability problems. In order to verify the validity of the artificial damping method, a truss structure was analyzed. Replacing the kinetic energy with the artificial damping energy makes it possible to analyze instability problems within the static analysis scheme. The proposed technique is useful not only for elastic local buckling problems but also for material-related instability problems.

6. References

1. Abaqus Users Manual, Dassault Systems Simulia Corp., 2013, Version 6.13, USA.
2. Esslinger, M., 1970, Hochgeschwindigkeitsaufnahmen von Beulvorgang dunnwandiger, axialbelasteter Zylinder, Der Stahlbau, 39 (3), 73-76.
3. Kobayashi, T., Mihara, Y. and Fujii, F., 2012, Path-Tracing Analysis for Post-buckling Process of Elastic Cylindrical Shells under Axial Compression, Thin-Walled Structures, 61, 180–187.
4. Kobayashi, T., Mihara, Y. and Fujii, F., 2016, Practical Methodology of Path-tracing Analysis for Buckling Process in Cylindrical Shells, Sixth International Conference on Structural Engineering, Mechanics and Computation.
5. Oide, K., Mihara, Y., Kobayashi, T. Takizawa, H., Amaishi, T. and Umezu, Y., 2016, Drawing simulation by static implicit analysis with the artificial damping method, Numisheet 2016, Journal of Physics: Conference Series 734.
6. Yamaki, N., 1984, Elastic Stability of Circular Cylindrical Shells, North-Holland, Netherlands, p.222.
7. Tateishi, J. and Nishiwaki, T., Imaging of polymer foam by three-dimensional computed tomography, SPring-8/SACLA Research Frontiers, 2011. , http://www.spring8.or.jp/pdf/en/res_fro/11/132-133.pdf
8. Phelps, N., B., Local and global deformation from synchrotron imaging of closed cell foams in compression, Oklahoma State University, 2005.